

ROBUST SPARSE MULTICHANNEL ACTIVE NOISE CONTROL

Jingli Xie¹, Danqi Jin¹, Wen Zhang^{1,2}, Xiao-Lei Zhang¹, Jie Chen¹, DeLiang Wang^{1,3}

¹Center for Intelligent Acoustics and Immersive Communications,
School of Marine Science and Technology, Northwestern Polytechnical University, China

²Research School of Engineering, College of Engineering and Computer Science
The Australian National University, Canberra, ACT 2601, Australia

³Department of Computer Science and Engineering, The Ohio State University, USA

ABSTRACT

Multichannel active noise control (MC-ANC) aims to cancel low-frequency noise in an enclosure. If noise sources are distributed sparsely in space, adding an ℓ_1 -norm constraint to the standard MC-ANC helps to reduce the complexity of the system and accelerate the convergence rate. However, the convergence performance of ℓ_1 -norm constrained MC-ANC ($c\ell_1$ -MC-ANC) degrades significantly in reverberant environments. In this paper, we analyze the necessity of using sparsity-inducing algorithms with distinct zero-attracting strengths over loudspeakers, and then derive three algorithms of this kind in the complex domain. Simulation results show that, compared to $c\ell_1$ -MC-ANC, the proposed algorithms exhibit faster convergence or higher noise reduction at steady state in both free field and reverberant environments.

Index Terms— Sparsity, ANC, convergence performance, robust

1. INTRODUCTION

Active noise control (ANC) is based on the principle of superposition, that is, a secondary noise with equal amplitude and opposite phase is introduced to counteract the primary noise [1, 2]. Multichannel active noise control (MC-ANC) is adopted to deal with noise in an enclosure, which requires multiple secondary sources and error sensors, as well as possible reference sensors depending on whether it is a feedforward [3–7] or feedback [8–10] structure. This paper focuses on the feedback MC-ANC where reference signals are not easily available.

In many applications of MC-ANC, using the secondary noise sources that are close to the primary noise sources is sufficient for noise control. This motivates the development of sparse MC-ANC [11, 12] for a common scenario that primary noise sources are sparsely distributed in space. In [11],

ℓ_1 -norm constrained MC-ANC ($c\ell_1$ -MC-ANC) is proposed to inactive the majority of the secondary sources and reduce the complexity of the system. Moreover, it exhibits faster convergence compared to the standard MC-ANC. However, it was only evaluated in the free field. When the sparsity condition is not strictly satisfied, for example in a mildly or even moderately reverberant environment, we find that its convergence performance significantly deteriorates, as shown later in Section 4. In $c\ell_1$ -MC-ANC, all the secondary sources are attracted to zero with the same strength, which can accelerate the convergence speed of near-zero sources, but introduces bias for large-valued sources. In the case of free field, near-zero sources are in the majority, thus bias is limited. While under reverberation conditions, the effect of reverberation can be represented by using a set of images [13], hence the sparsity of the secondary sources is reduced and more sources tend to have large values. In this case, shrinking all sources uniformly will introduce significant bias and make $c\ell_1$ -MC-ANC suffer from high steady state residual energy.

Motivated by research on sparse system identification [14–16], this paper proposes three kinds of sparsity constrained MC-ANCs to improve the robustness in reverberant environments. Essentially, we employ a reweighted zero attractor for each secondary source, that is, only loudspeakers with small outputs are shrunk to zero. Simulation results show that the proposed algorithms exhibit faster convergence or higher noise reduction at steady state in both free field and reverberant environments.

The remainder of this paper is organized as follows. In Section 2, we formulate the problem of feedback MC-ANC. We describe our proposed algorithms in Section 3. The simulation setup and evaluation results are presented in Section 4. We conclude this paper in Section 5.

2. BACKGROUND

Let the desired quiet region Q be a circular zone with radius R_1 and a noise source is located outside of this region as shown in Fig. 1. A uniform circular array, composed of M

Email: yetixie1994@mail.nwpu.edu.cn

This work was supported in part by the National Natural Science Foundation of China (NSFC) funding scheme under Project No. 61671380, No. 61671381 and No. 61671382.

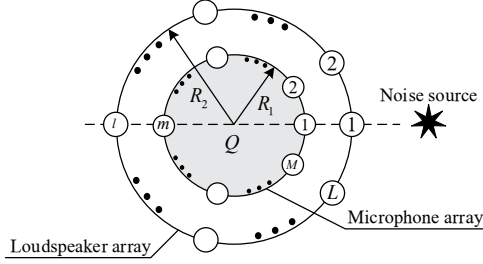


Fig. 1. Multichannel feedback ANC.

microphones, is placed along the boundary of the region to pick up residual signals. A uniform concentric circular array with radius R_2 ($R_2 > R_1$), consisting of L loudspeakers, is placed outside of the region Q to generate secondary signals.

In the frequency domain, residual signals recorded by error microphones can be written as

$$\epsilon(f) = \mathbf{p}(f) + \mathbf{H}\mathbf{d}(f), \quad (1)$$

where error signals ϵ , primary signals \mathbf{p} are vectors of length M , the driving signal of loudspeakers \mathbf{d} is a vector of length L , \mathbf{H} is an $M \times L$ matrix to represent the acoustic transfer functions (ATFs), and f is frequency.

In order to minimize the total energy of the residual signals, the cost function $J(n)$ in the standard MC-ANC is defined as $J(n) = \frac{1}{2}\epsilon^H(n)\epsilon(n)$, where superscript $(\cdot)^H$ denotes complex conjugate transpose and n is the number of iteration. Note that for convenience, frequency f is not shown.

In the $c\ell_1$ -MC-ANC [11], a new cost function $J_{\ell_1}(n)$ is defined by incorporating a complex ℓ_1 -norm penalty, that is,

$$J_{\ell_1}(n) = \frac{1}{2}\epsilon^H(n)\epsilon(n) + \lambda\|\mathbf{d}(n)\|_1, \quad (2)$$

where $\lambda \geq 0$ is a regularization parameter to balance the residual energy and the sparsity of driving signals, and $\|\cdot\|_1$ denotes the ℓ_1 -norm of a complex-valued vector.

3. PROPOSED ALGORITHMS

3.1. Problem formulation

Instead of using the ℓ_1 -norm, properly designing a sparsity-inducing term can be beneficial in many settings [14–18]. We then write a general form of (2) as

$$J(n) = \frac{1}{2}\epsilon^H(n)\epsilon(n) + \lambda\Omega(\mathbf{d}(n)) \quad (3)$$

where $\Omega(\mathbf{d}(n))$ can be any sparse regularization term. By minimizing (3) using the gradient descent method, the driving signals are updated as

$$\mathbf{d}(n+1) = \mathbf{d}(n) - 2\mu\nabla_{\mathbf{d}}J(n), \quad (4)$$

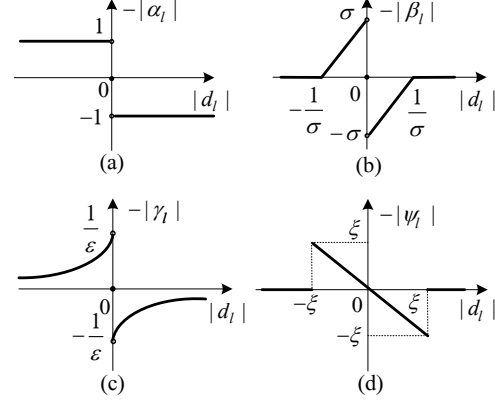


Fig. 2. Zero-attractors of (a) $c\ell_1$ -MC-ANC (b) Q - $c\ell_0$ -MC-ANC (c) R - $c\ell_1$ -MC-ANC (d) C - $c\ell_2$ -MC-ANC.

where $\mu > 0$ is the step size, and $\nabla_{\mathbf{d}}J(\cdot)$ denotes the gradient of $J(\cdot)$ with respect to the complex vector \mathbf{d} .

As a special case, the gradient of $J_{\ell_1}(n)$ is derived using Wirtinger calculus [19] as

$$\nabla_{\mathbf{d}}J_{\ell_1}(n) = \frac{1}{2}[\mathbf{H}^H\epsilon(n) + \lambda\boldsymbol{\alpha}(n)] \quad (5)$$

where $\boldsymbol{\alpha}(n)$, called *zero-attractor*, is an $L \times 1$ vector with the l th entry given by

$$\alpha_l(n) = \begin{cases} \frac{d_l(n)}{|d_l(n)|}, & |d_l(n)| \neq 0 \\ 0, & |d_l(n)| = 0 \end{cases}, \quad (6)$$

where $|\cdot|$ denotes the modulus of its complex argument, $\alpha_l(n)$ and $d_l(n)$ denote the l -th entries of $\boldsymbol{\alpha}(n)$ and $\mathbf{d}(n)$, respectively.

The relation between α_l and $|d_l|$ is shown in Fig. 2(a). It is observed that the zero-attractors of the $c\ell_1$ -MC-ANC shrink all entries of \mathbf{d} uniformly, which may result in a significant bias if the sparsity of the secondary sources is reduced.

3.2. Proposed sparsity constrained algorithms

To enhance robustness against reverberation, here we introduce three new regularization terms $\Omega(\mathbf{d}(n))$, which only shrink small-valued sources and avoid introducing significant bias. As will be shown in the simulation part, each of these regularization terms has its own favorable properties, and can be used accordingly in different environments.

3.2.1. Quasi complex ℓ_0 -norm MC-ANC

The quasi ℓ_0 -norm constrained LMS is proposed in [16], but is restricted to the real-valued case. In this paper, we extend it to the MC-ANC with complex-valued operations. The quasi complex ℓ_0 -norm constrained MC-ANC (Q - $c\ell_0$ -MC-ANC) is

derived via

$$J_{\ell_0}(n) = \frac{1}{2} \boldsymbol{\epsilon}^H(n) \boldsymbol{\epsilon}(n) + \lambda \sum_{l=1}^L (1 - e^{-\sigma |d_l(n)|}), \quad (7)$$

where $\sigma > 0$ controls the shrinkage range and strength. The gradient of $J_{\ell_0}(n)$ is

$$\nabla_{\mathbf{d}} J_{\ell_0}(n) = \frac{1}{2} [\mathbf{H}^H \boldsymbol{\epsilon}(n) + \lambda \boldsymbol{\beta}(n)], \quad (8)$$

where $\boldsymbol{\beta}(n)$ is an $L \times 1$ vector with the l th entry given by

$$\beta_l(n) = \begin{cases} \sigma e^{-\sigma |d_l(n)|} \frac{d_l(n)}{|d_l(n)|}, & |d_l(n)| \neq 0 \\ 0, & |d_l(n)| = 0 \end{cases}, \quad (9)$$

with $\beta_l(n)$ being the l th entry of $\boldsymbol{\beta}(n)$. Further, we adopt a first-order Taylor expansion to approximate the exponential term in (9) as in [16] to reduce the computational complexity, which leads to

$$e^{-\sigma |d_l(n)|} \approx \begin{cases} 1 - \sigma |d_l(n)|, & |d_l(n)| < 1/\sigma \\ 0, & \text{otherwise} \end{cases}. \quad (10)$$

Visualizing the zero attractors of (9) in Fig. 2(b), it is clear that the Q-cl₀-MC-ANC does not shrink large $d_l(n)$.

3.2.2. Reweighted complex ℓ_1 -norm MC-ANC

Motivated by previous works in system identification [14, 15], we propose a reweighted complex ℓ_1 -norm constrained MC-ANC (R-cl₁-MC-ANC), with the cost function defined by

$$J_{\text{R}}(n) = \frac{1}{2} \boldsymbol{\epsilon}^H(n) \boldsymbol{\epsilon}(n) + \lambda \sum_{l=1}^L \log[1 + |d_l(n)|/\varepsilon], \quad (11)$$

where the positive parameter ε controls the shrinkage range. The log-sum penalty $\sum_{l=1}^L \log[1 + |d_l(n)|/\varepsilon]$ is considered, as it behaves more similarly to the ℓ_0 -norm than to $\|\mathbf{d}(n)\|_1$ [20]. The derivative of $J_{\text{R}}(n)$ is

$$\nabla_{\mathbf{d}} J_{\text{R}}(n) = \frac{1}{2} [\mathbf{H}^H \boldsymbol{\epsilon}(n) + \lambda \boldsymbol{\gamma}(n)], \quad (12)$$

with the l th entry of $\boldsymbol{\gamma}(n)$ given by

$$\gamma_l(n) = \begin{cases} \frac{1}{|d_l(n)| + \varepsilon} \cdot \frac{d_l(n)}{|d_l(n)|}, & |d_l(n)| \neq 0 \\ 0, & |d_l(n)| = 0 \end{cases}. \quad (13)$$

The property of $\gamma_l(n)$ is shown in Fig. 2(c), which shrinks less to larger $d_l(n)$.

3.2.3. Clipped complex ℓ_2 -norm MC-ANC

It is obvious that both Q-cl₀-MC-ANC and R-cl₁-MC-ANC are dedicated to avoid introducing bias for d_l with large values. However, for d_l with small values, the shrinkage strength

Table 1. Hyperparameter Settings.

	free field				reverberant field					
	μ	λ	σ	ε	ξ	μ	λ	σ	ε	ξ
MC-ANC	5	-	-	-	-	4	-	-	-	-
cl ₁ -MC-ANC	5	0.01	-	-	-	4	0.02	-	-	-
Q-cl ₀ -MC-ANC	5	0.02	0.5	-	-	4	0.05	0.25	-	-
R-cl ₁ -MC-ANC	5	0.02	-	2.2	-	4	0.05	-	3	-
C-cl ₂ -MC-ANC	5	0.02	-	-	2	4	0.05	-	-	1

is preferably proportional to the value of $|d_l|$. Based on this, we propose a clipped complex ℓ_2 -norm MC-ANC (C-cl₂-MC-ANC), that is,

$$J_{\text{C}}(n) = \frac{1}{2} \boldsymbol{\epsilon}^H(n) \boldsymbol{\epsilon}(n) + \frac{\lambda}{2} \sum_{l=1}^L \min\{d_l^2(n), \xi^2\}, \quad (14)$$

where $\xi > 0$ is a predefined threshold used to control the shrinkage range, and $\min\{\cdot, \cdot\}$ denotes the minimum operator. The gradient of $J_{\text{C}}(n)$ is

$$\nabla_{\mathbf{d}} J_{\text{C}}(n) = \frac{1}{2} [\mathbf{H}^H \boldsymbol{\epsilon}(n) + \lambda \boldsymbol{\psi}(n)], \quad (15)$$

with the l th entry of $\boldsymbol{\psi}(n)$ derived as

$$\psi_l(n) = \begin{cases} d_l(n), & |d_l(n)| < \xi \\ 0, & \text{otherwise} \end{cases}. \quad (16)$$

The property of $\psi_l(n)$ is illustrated in Fig. 2(d).

4. SIMULATION

4.1. Simulation setup

Assume that the desired quiet zone Q is a circular region with a radius of 1 m. We place 11 microphones equally along the boundary of the region Q to pick up residual signals, and 11 loudspeakers equally on a concentric circle with a radius of 2 m to generate secondary signals. A primary noise source is located 2.5 m away from the circle center at the same height, and its magnitude and frequency are 10 and 200 Hz, respectively. As in [11], we assume that both the noise source and loudspeakers as cylindrical wave sources, and white Gaussian noise with SNR of 40 dB is added to each microphone recordings to model internal thermal noise or measurement errors. The speed of sound is $c = 343$ m/s.

To mimic a moderate reverberation environment, we generate a simulated room with size 6 m \times 5 m (length \times width) using the image source method [20]. The center of the room coincides with the center of the loudspeaker/microphone array. The ceiling and floor are perfectly absorbing and all side walls have a reflection coefficient of 0.5.

All parameters used in the algorithms are listed in Table 1. We evaluate the performance according to the noise reduction (NR) at the position of error microphones $[\text{NR}_{\text{mic}}(n)]$ and

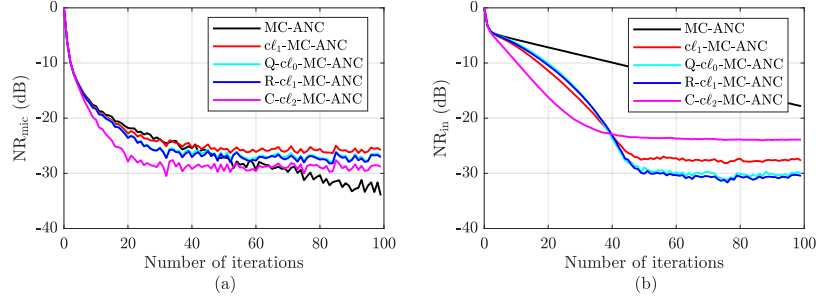


Fig. 3. Analysis of the convergence speed and noise reduction ability of the compared methods in a free field environment. (a) $NR_{mic}(n)$, (b) $NR_{in}(n)$.

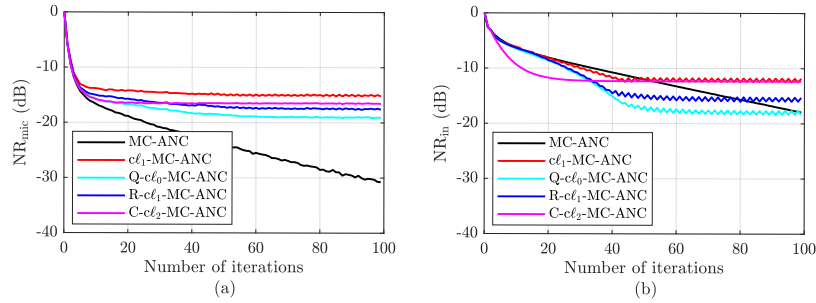


Fig. 4. Analysis of the convergence speed and noise reduction ability of the compared methods in a reverberant environment. (a) $NR_{mic}(n)$, (b) $NR_{in}(n)$.

noise reduction inside the control region [$NR_{in}(n)$] as in [11]. For the latter, 1296 sampling points are uniformly chosen in the control region to evaluate the system performance.

4.2. Results

Figure 3 illustrates the convergence performance of all algorithms in the free field. It is observed that, compared to MC-ANC, all sparsity-constrained ANC algorithms increase the convergence rate, especially for noise reduction inside the region as shown in Fig. 3(b). For the sparsity-constrained ANC algorithms, the proposed $Q-cl_0$ -MC-ANC and $R-cl_1$ -MC-ANC have similar convergence speed compared to cl_1 -MC-ANC, but have higher noise reduction at steady state. Among all these algorithms, $C-cl_2$ -MC-ANC has the fastest convergence rate but least noise reduction at steady state, which is preferable for rapidly-changing environments.

We then evaluate the performance of all above algorithms in the case of a reverberant environment, and the results are shown in Fig. 4. In Fig. 4(a) for $NR_{mic}(n)$, MC-ANC has the best performance and all sparsity-promoting algorithms prematurely reach steady state. Inside the control region, Fig. 4(b) shows that, the cl_1 -MC-ANC has a particularly high misadjustment at steady state due to the bias introduced by ℓ_1 -norm, and shows almost no advantage over MC-ANC. All proposed sparsity-constrained algorithms have larger noise reduction at steady state than cl_1 -MC-ANC and exhibit faster

convergence than MC-ANC, which is a favorable property for an adaptive system. Among the proposed algorithms, $Q-cl_0$ -MC-ANC and $R-cl_1$ -MC-ANC have higher noise reduction at steady state, while $C-cl_2$ -MC-ANC has faster convergence. This suggests that the selection of $Q-cl_0$ -MC-ANC, $R-cl_1$ -MC-ANC, or $C-cl_2$ -MC-ANC depends on the degree of nonstationarity of the environment. The $C-cl_2$ -MC-ANC is preferable for a rapidly-changing environment and $Q-cl_0$ -MC-ANC is a better choice for a relatively stable environment.

5. CONCLUSION

In this paper, we proposed three kinds of sparse MC-ANC algorithms, called $Q-cl_0$ -MC-ANC, $R-cl_1$ -MC-ANC, and $C-cl_2$ -MC-ANC, to improve the robustness of MC-ANC in reverberant environments when noise sources are sparsely distributed in space. Compared to the existing cl_1 -MC-ANC algorithm, the proposed algorithms selectively shrink those secondary sources with small outputs. Simulation results demonstrated the effectiveness of the proposed algorithms in both free field and reverberant environments, in terms of both noise reduction ability and convergence speed. Our future work includes finding a systematic way to choose model parameters and investigate the variable-parameter method to further improve the robustness.

6. REFERENCES

- [1] S. M. Kuo and D. R. Morgan, *Active noise control systems: algorithms and DSP implementations*. John Wiley & Sons, Inc., 1995.
- [2] Y. Kajikawa, W.-S. Gan, and S. M. Kuo, "Recent advances on active noise control: open issues and innovative applications," *APSIPA Trans. Sig. Inf. Process.*, vol. 1, pp. 1–21, Aug. 2012.
- [3] S. J. Elliott, I. Stothers, and P. Nelson, "A multiple error LMS algorithm and its application to the active control of sound and vibration," *IEEE Trans. Acoust., Speech, Signal Process.*, vol. 35, pp. 1423–1434, Oct. 1987.
- [4] F. Borchì, M. Carfagni, L. Martelli, A. Turchi, and F. Argenti, "Design and experimental tests of active control barriers for low-frequency stationary noise reduction in urban outdoor environment," *Appl. Acoust.*, vol. 114, pp. 125–135, Dec. 2016.
- [5] K. Tanaka, C. Shi, and Y. Kajikawa, "Multi-channel active noise control using parametric array loudspeakers," in *APSIPA Trans. Sig. Inf. Process.*, pp. 1–6, Dec. 2014.
- [6] T. Kosaka, S. J. Elliott, and C. C. Boucher, "A novel frequency domain filtered-x LMS algorithm for active noise reduction," in *Proc. IEEE ICASSP*, vol. 1, pp. 403–406, 1997.
- [7] J. Lorente, M. Ferrer, M. De Diego, and A. González, "GPU implementation of multichannel adaptive algorithms for local active noise control," *IEEE Trans. Audio, Speech, Lang. Process.*, vol. 22, pp. 1624–1635, Nov. 2014.
- [8] S. M. Kuo, X. Kong, and W. S. Gan, "Applications of adaptive feedback active noise control system," *IEEE Trans. Contr. Syst. Technol.*, vol. 11, pp. 216–220, Mar. 2003.
- [9] T. Meurers, S. M. Veres, and S. J. Elliott, "Frequency selective feedback for active noise control," *IEEE Control Syst.*, vol. 22, pp. 32–41, Aug. 2002.
- [10] L. Luo, J. Sun, and B. Huang, "A novel feedback active noise control for broadband chaotic noise and random noise," *Appl. Acoust.*, vol. 116, pp. 229–237, Jan. 2017.
- [11] J. Zhang, T. D. Abhayapala, P. N. Samarasinghe, W. Zhang, and S. Jiang, "Multichannel active noise control for spatially sparse noise fields," *J. Acoust. Soc. Am.*, vol. 140, pp. EL510–EL516, Nov. 2016.
- [12] J. Zhang, T. D. Abhayapala, P. N. Samarasinghe, W. Zhang, and S. Jiang, "Sparse complex FxLMS for active noise cancellation over spatial regions," in *Proc. IEEE ICASSP*, pp. 524–528, 2016.
- [13] P. A. Naylor and N. D. Gaubitch, Eds, *Speech dereverberation*. Springer Science & Business Media, 2010.
- [14] Y. Chen, Y. Gu, and A. O. Hero, "Sparse LMS for system identification," in *Proc. IEEE ICASSP*, pp. 3125–3128, 2009.
- [15] D. Jin, J. Chen, C. Richard, and J. Chen, "Model-driven online parameter adjustment for zero-attracting LMS," *Signal Process.*, vol. 152, pp. 373–383, Nov. 2018.
- [16] Y. Gu, J. Jin, and S. Mei, " ℓ_0 norm constraint LMS algorithm for sparse system identification," *IEEE Signal Process. Lett.*, vol. 16, pp. 774–777, Jun. 2009.
- [17] R. Tibshirani, "Regression shrinkage and selection via the lasso," *J. Roy. Statist. Soc. B, Methodol.*, vol. 58, pp. 267–288, Feb. 1996.
- [18] D. Jin, J. Chen, C. Richard, and J. Chen, "Adaptive parameters adjustment for group reweighted zero-attracting LMS," in *Proc. IEEE ICASSP*, pp. 4294–4298, 2018.
- [19] S. Haykin, *Adaptive filter theory*. Pearson Education India, 2008.
- [20] J. B. Allen and D. A. Berkley, "Image method for efficiently simulating small-room acoustics," *J. Acoust. Soc. Am.*, vol. 65, pp. 943–950, Jun. 1979.